CROATICA CHEMICA ACTA CCACAA **74** (2) 359–380 (2001)

ISSN-0011-1643
CCA-2737 *Original Scientific Paper*

Preparation, Thermal Analysis and Spectral Characterization of the 1:1 Complexes of Mercury(II) Halides and Pseudohalides with 3,4,5,6-Tetrahydropyrimidine-2-thione. Crystal Structures of Bis(3,4,5,6-tetrahydropyrimidine-2-thione-*S*)mercury(II) Tetrachloro and Tetrabromomercurate(II)

Zora Popović, [a,*] *Dubravka Matković-Čalogović,*[a] *Gordana Pavlović,*[a] *Željka Soldin,*[a] *Gerald Giester,*[b] *Maša Rajić,*[c] *and Dražen Vikić-Topić*[d]

[a]*Laboratory of General and Inorganic Chemistry, Faculty of Science, Chemistry Department, University of Zagreb, Ul. kralja Zvonimira 8, 10000 Zagreb, Croatia*

[b]*Institut für Mineralogie und Kristallographie, Geozentrum, Universität Wien, Althanstraße 14, A-1090 Wien, Austria*

[c]*Laboratory for Thermal Analysis, Brodarski Institute – Marine Research and Special Technology, Av. V. Holjevca 20, 10000 Zagreb, Croatia*

[d]*Ruđer Bošković Institute, NMR Centre, P. O. Box 180, HR-10002 Zagreb, Croatia*

Received October 16, 2000; revised December 22, 2000; accepted December 22, 2000

Mercury(II) complexes of the type $HgX_2(H_4pymtH)$ (X = Cl^-, Br^-, I^-, SCN^-, CN^-; H_4pymtH = 3,4,5,6-tetrahydropyrimidine-2-thione) have been obtained and structurally characterized by X-ray diffraction, IR, ^1H and ^{13}C NMR spectroscopy. Single crystal X-ray structure analysis was performed for the chloro and bromo complexes, which were found to be isostructural. Their crystal structures consist of $[Hg(H_4pymtH)_2]^{2+}$ complex cations and $[HgX_4]^{2-}$ complex anions interconnected by Hg···X contacts into puckered sheets. The crystal structure of H_4pymtH has been redetermined to greater

* Author to whom correspondence should be addressed. (E-mail: zpopovic@chem.pmf.hr)

accuracy. In solution NMR spectra of complexes, the greatest complexation effects were found on the ^{13}C chemical shift of the thioketo-carbon atom and on the ^{1}H chemical shift of the NH protons.

Key words: mercury(II) complexes, heterocyclic thiones, crystal structure, thermal analysis, ^{1}H and ^{13}C NMR spectra.

INTRODUCTION

Mercury mostly forms covalent complexes with different proteins by binding particularly to S-donor groups (cysteine thiol) or, if these are not available, to N- or O- donor groups. The way of binding also depends on the strength of the mercury-ligand bond in the mercury compound reacting with the protein.[1] We are interested in characterizing mercury complexes with bonds to S-donor ligands which can be used as models for a better understanding of mercury binding in biological systems. In order to get more information on the role of halides and pseudohalides in such systems, more information on the competition of halides and pseudohalides with such binding sites is needed. It has been reported that an excess of chloride ions could compete with the binding sites by complexing mercury.[1] On the other hand, there are two types of complexes of $HgCl_2$ with L-cysteine, one with covalently bonded chlorine and sulphur atoms that can be, in hot water, converted into the other complex with ionic chloride ions and stronger Hg–S bonds.[2] A survey of the solvation of mercury(II) halides in 80 solvents, including several S-donor solvents, shows complex formation properties with ligands of different electron-pair donor properties.[3] The thermodynamics and structural properties of the complex formation in aqueous and non-aqueous solutions have been reported.[4–13]

The great structural variety of complexes of mercury halides and pseudohalides with different S-donor ligands reflects the flexibility of the mercury coordination geometry. A series of studies on the interaction of mercury(II) salts with various heterocyclic thiones, both in the solid state and in solution, have been performed in order to get more information on the competition processes.[14–24] We have recently reported synthetic, spectroscopic, thermoanalytical and crystal structure studies of the 1:2 complexes of mercury(II) halides (Cl^-, Br^- and I^-) and pseudohalides (SCN^-, CN^-) with H_4pymtH.[25] We have chosen methanol as a poor oxygen donating solvent toward mercury(II) salts to examine the influence of the stoichiometric ratio of mercury(II) halides and pseudohalides on the complex formation with H_4pymtH, which is a strong S-donor. Here we report characterization of the 1:1 complexes with the same ligand.

Structures of the 1:1 complexes of mercury(II) halides or pseudohalides with various neutral ligands in the solid state show that they often consist of discrete halogen-bridged dimeric molecules with mercury atom in a deformed tetrahedral environment. This cannot be assumed for all 1:1 complexes, since other more associated structures are also known.[26–29] The structural chemistry of these complexes is thus difficult to systematize.

EXPERIMENTAL

Reagents and Apparatus

Mercury(II) halides and cyanide as well as the ligand (H4pymtH) were obtained from Aldrich and used without further purification. Mercury(II) thiocyanate was prepared by the reaction of mercury(II) nitrate monohydrate and ammonium thiocyanate. The mercury content of the compounds was determined by the complexometric titration with sodium diethyldithiocarbamate of the solution obtained after decomposition of the specimen in *aqua regia*.[30] N and S analyses were provided by the Analytical Services Laboratory of the Ruđer Bošković Institute. The IR spectra were recorded as KBr pellets on a Perkin-Elmer FTIR 1600 spectrometer over the range 4000–450 cm^{-1}. Thermal measurements were performed using a simultaneous TGA-DTA analyser (TA Instruments, SDT Model 2960). Samples were placed into small aluminium oxide sample pans. The TGA and DTA curves were obtained by placing the samples of about 5 mg into open sample pans at a heating rate of 10 °C min^{-1} and nitrogen (purity above 99.996%) pouring at a flow rate of 50 mL min^{-1}. The SDT was calibrated with indium.

The ^{1}H and ^{13}C NMR spectra were measured on a Varian Gemini 300 spectrometer, operating at 75.46 MHz for the ^{13}C nucleus. Samples were dissolved in DMSO-d_6 in 5 mm NMR tubes. Concentrations were 0.05 mol dm^{-3} for ^{1}H and 0.25 mol dm^{-3} for ^{13}C measurements. Spectra were recorded at 20 °C. Chemical shifts (ppm) were referred to TMS. Digital resolution was 0.32 Hz per point in ^{1}H and 0.70 Hz per point in ^{13}C NMR one-dimensional spectra. The following techniques were used: standard ^{1}H, ^{13}C broadband proton decoupled, ^{13}C gated decoupled, COSY45 and NOESY. The Waltz-16 sequence was used for proton decoupling. The COSY45 spectra were measured in the magnitude mode with 1024 points in F2 dimension and 256 increments in F1 dimension, the latter zero-filled to 1024 points. Each increment was taken with 16 scans, 5000 Hz spectral width and a relaxation delay of 0.8 s. The corresponding digital resolution was 9.8 Hz/point and 19.5 Hz/point in F2 and F1 dimensions, respectively. NOESY spectra were recorded in the phase-sensitive mode with a mixing time of 0.5 s, while other parameters were as in COSY spectra.

Synthesis and Characterization of Complexes

General Procedure

The complexes were prepared by adding dropwise a methanol solution of the thione ligand to an equimolar methanol solution of the appropriate mercury(II) halide or pseudohalide. The crystalline solids, which were formed after standing for

TABLE I

General and crystal data and summary of intensity data collection and structure refinement

Compound	**1**	**2**	H_4pymtH
Formula	$C_{16}H_{32}Cl_8Hg_4N_8S_4$	$C_{16}H_{32}Br_8Hg_4N_8S_4$	$C_4H_8N_2S$
M_r	1550.70	1906.38	116.19
Crystal system and form	Triclinic, prism	Triclinic, prism	Orthorhombic, prism
Space group	$P\bar{1}$	$P\bar{1}$	*Cmca*
Crystal dimensions / mm^3	0.52 × 0.46 × 0.10	0.42 × 0.36 × 0.22	0.41 × 0.38 × 0.22
a / Å	10.0451(15)	10.439(3)	8.380(3)
b / Å	13.530(2)	13.749(2)	15.045(5)
c / Å	14.1620(17)	14.500(3)	9.334(3)
α / °	103.008(13)	102.6970(17)	
β / °	91.997(15)	92.082(2)	
γ / °	90.34(2)	90.1747(19)	
V / $Å^3$	1874.1(5)	2028.7(8)	1176.8(7)
Z	2	2	8
D_c / g cm^{-3}	2.748	3.121	1.312
μ / mm^{-1}	17.151	23.196	0.4
F (000)	1408	1696	496
2 θ range for data collection / °	2.37 to 27.03	3.04 to 29.97	3.5 to 30.0
h,k,l range	–12 to 12, –17 to16, 0 to18	–14 to 14, –19 to 18, 0 to 20	–3 to 11, –5 to 21, 0 to 13
Scan type	ω	ω	ω

Face indices, distances from centroid / mm	(0 1 0), (0 –1 0) 0.050	(0 1 0), (0 –1 0) 0.1090	
	(1 0 1), (–1 0 –1) 0.263	(1 0 1) 0.205; (–1 0 –1) 0.195	
	(1 0 –1), (–1 0 1) 0.230	(–1 0 1) 0.165; (0 –1 –1) 0.155	
		(1 0 0) 0.200; (–1 0 0) 0.215	
		(1 1 1) 0.178; (–1 –1 –1) 0.182	
		(1 –1 1) 0.190; (–3 1 4) 0.165	
Range of transmission factors, min., max.[a]	0.0096, 0.1753	0.0117, 0.0633	
No. measured reflections	12338	11640	1555
No. independent reflections (R_{int})	8036 (R_{int} = 0.053)	11215 (R_{int} = 0.066)	877 (R_{int} = 0.057)
No. refined parameters	371	362	41
No. observed reflections, $I \geq 2\sigma(I)$	5474	4927	596
g_1, g_2 in w[b]	0.1017, 0	0.0877, 0	0.0728, 0
R[c], wR[d] [$I \geq 2\sigma(I)$]	0.0582, 0.1319	0.0589, 0.1272	0.0298, 0.076
R, wR [all data]	0.0933, 0.1496	0.1615, 0.1665	0.0584, 0.088
Goodness of fit on F^2, S[e]	0.991	0.900	0.80
Max., min. electron density / (e Å^{-3})[f]	2.264, –4.266	2.305, –2.753	0.23, –0.18
Extinction coefficient	0.0010(2)	0.0049(2)	
Maximum Δ / σ	0.001	0.001	< 0.001

[a] Absorption correction type: numerical Gaussian. [b] $w = 1 / [\sigma^2(F_o^2) + [g_1P + g_2P]$ where $P = (F_o^2 + 2F_c^2) / 3$. [c] $R = \Sigma \left||F_o| - |F_c|\right| / \Sigma |F_o|$. [d] $wR =$ $= [\Sigma (F_o^2 - F_c^2)^2 / \Sigma w (F_o^2)^2]^{1/2}$; [e] $S = \Sigma [w(F_o^2 - F_c^2)^2 / (N_{obs} - N_{param})]^{1/2}$. [f] In all structures, the max. electron density in the last difference Fourier map is near Hg.

several days, were filtered off, washed with methanol and dried. The isolated complexes are crystalline and colourless substances, except the iodo complex which is yellow. The thiocyanato complex is photosensitive and should be kept in dark. All of the complexes are generally insoluble in common organic solvents but soluble in solvents of pronounced donor properties such as DMSO, DMF, γ-picoline or pyridine. All attempts to obtain a compound with mercury(II) acetate have failed so far, *i.e.* decomposition to elementary mercury occurs.

*Preparation of $HgCl_2(H_4pymtH)$ (**1**)*

Yield: 89%. *Anal.* Calcd. for $C_4H_8Cl_2HgN_2S$ (M_r = 387.69): N 7.22, S 8.27, Hg 51.75%; found: N 7.35, S 8.20, Hg 51.83%.

*Preparation of $HgBr_2(H_4pymtH)$ (**2**)*

Yield: 83%. *Anal.* Calcd. for $C_4H_8Br_2HgN_2S$ (M_r = 476.59): N 5.88, S 6.73, Hg 42.10%; found: N 5.88, S 6.78, Hg 42.36%.

*Preparation of $HgI_2(H_4pymtH)$ (**3**)*

Yield: 60%. *Anal.* Calcd. for $C_4H_8I_2HgN_2S$ (M_r = 570.59): C 8.41, H 1.40, N 4.90%; found: C 8.63, H 1.63, N 5.10%.

*Preparation of $Hg(SCN)_2(H_4pymtH)$ (**4**)*

Yield: 62%. *Anal.* Calcd. for $C_8H_8HgN_4S_3$ (M_r = 432.94): N 12.94, S 22.22, Hg 46.34%; found: N 13.08, S 22.28, Hg 46.52%.

*Preparation of $Hg(CN)_2(H_4pymtH)$ (**5**)*

Yield: 31%. *Anal.* Calcd. for $C_6H_8HgN_4S$ (M_r = 368.82): N 15.19, S 8.70, Hg 54.40%; found: N 15.21, S 8.73, Hg 54.44%.

Data Collection and Structure Determination

Single crystal X-ray diffraction data were collected for H_4pymtH and for complexes **1** and **2** using Mo-Kα radiation (graphite monochromator). The structure of H_4pymtH was redetermined to greater accuracy than the one reported previously.[31] Crystal data, experimental conditions, details of structure determination and final refinement parameters are given in Table I. Data for H_4pymtH and complexes **1** and **2** were collected at room temperature on the Philips PW1100 diffractometer. The unit-cell parameters were derived by the least-squares refinement (STADI4 program)[32] of 59 ($11.6 \leq \theta \leq 17.3°$), 45 ($10.1 \leq \theta \leq 19.0°$) and 32 reflections ($10.5 \leq \theta \leq 17.0°$) for H_4pymtH and for complexes **1** and **2**. Standard reflections, monitored every 1.5 h, showed an intensity variation of ± 5.5% for H_4pymtH, ± 2.6% for **1** and ± 1.0% for **2**. Intensities were corrected for decay, Lorentz, polarization and absorption effects by the X-RED program.[33] Numerical absorption correction was performed for **1** and **2** using distances from the centroid to the crystal faces. The structures were solved by direct methods (H_4pymtH in a different space group setting than in the literature)[31] and completed by Fourier syntheses. Full matrix least-squares anisotropic refinement of non-hydrogen atoms based on F^2 against all reflections was applied.

A positional disorder of atom C23 was observed in **1**. The occupancy factor refinement for the two possible atom positions gave values of 0.75(3) and 0.25(3). All hydrogen atoms were generated at idealized geometrical positions (Nsp^2–H 0.86 Å; Csp^3–H 0.97 Å; U_{iso} = 1.2 U_{eq} for Nsp^2, 1.5 for Csp^3) and included in the refinement using the riding model, except for the nitrogen H atoms in H_4pymtH which were found

in the difference Fourier map and were isotropically refined. The hydrogen atoms belonging to the disordered atom C23 in **1** were generated with the corresponding occupancy factors. All calculations were perfomed by SHELXS,[34] and SHELXL97;[35] molecular graphics was done by PLATON98.[36]

RESULTS AND DISCUSSION

IR Spectra

Characteristic infrared bands in the spectra of the thione molecule (H_4pymtH) and its mercury(II) complexes **1–5** are presented in Table II. The principal IR bands of H_4pymtH were discussed in our previous work.[25] In the spectra of all complexes, a small upward shift of the coupled vibrations of C–N stretching and N–H bending was observed, which is consistent with an increase in the C–N bond order. The N–H out of plane vibrations were shifted to lower frequencies by *ca.* 80–100 cm^{-1} for the halide, and 25–50 cm^{-1} for the pseudohalide complexes, pointing at possible structural differences. In complexes **1–5**, the C–S stretching was shifted to lower frequencies due to the weakening of the C–S bond. The ν(C≡N) stretching vibrations in $Hg(SCN)_2(H_4$pymtH) were observed at 2135, 2115 and 2084 cm^{-1}, which is consistent with the presence of the bridging and terminal thiocyanate. The

TABLE II

Characteristic IR bands / cm^{-1} and their assignments[a]

	ν NH	ν_aC–N+ δ NH	δ NH+ ν_aC–N	δ NH+ ν_sC–N	w CH_2	π NH	ν C=S
H_4pymtH	3158s,br 3099s	1563vs	1554vs	1208vs	1193s	768s,br	644s
$HgCl_2(H_4$pymtH) (**1**)	3252s,br 3158m	1615s	1562s	1232s	1202m	689m,br	617m
$HgBr_2(H_4$pymtH) (**2**)	3300vs,br 3113s	1606vs	1564vs	1232vs	1202s	672s	600s,br[b]
$HgI_2(H_4$pymtH) (**3**)	3322s,br	1594s	1555vs	1212s	1198m-s	661m	600s,br[b]
$Hg(SCN)_2(H_4$pymtH) (**4**)	3221s,br 3114m	1594s 1575s	1561s	1240m-s	1208m	737m,br 716m,br	621m
$Hg(CN)_2(H_4$pymtH) (**5**)	3372vs 3227s,br	1617vs 1566vs,br	1558vs,br	1230s	1208vs	751m	600m

[a] Abbreviations: ν_a – asymmetric stretching; ν_s – symmetric stretching; δ – in plane bending; π – out of plane bending; w – wagging; vs – very strong; s – strong; m – medium; br – broad.

[b] Broad band (~ 40 cm^{-1}) centered at 600 cm^{-1}.

frequency of $\nu(C\equiv N)$ is usually higher in the bridging thiocyanates than in the ones that are terminally bonded but factors such as coordination number or stereochemistry of the complex may also effect this frequency. In the IR spectrum of $Hg(CN)_2(H_4pymtH)$, $\nu(C\equiv N)$ was observed at 2175 cm^{-1}, which is very similar to the structure of free $Hg(CN)_2$.[37]

*Crystal Structures of [Hg(H$_4$pymtH)$_2$][HgX$_4$] (X = Cl$^-$(**1**), Br$^-$(**2**))*

The 1:2 complexes of HgX_2 (X = Cl^-, Br^- and I^-) with H_4pymtH were all monomeric with tetrahedral coordination of Hg (two S-bound H_4pymtH and two halide ligands).[25] The structures of the 1:1 complexes are quite different. The complexes bis(3,4,5,6-tetrahydropyrimidine-2-thione-*S*)mercury(II) tetrachloromercurate (**1**) and tetrabromomercurate (**2**) are isostructural. Their asymmetric units contain two crystallographically independent $[Hg(H_4pymtH)_2]^{2+}$ cations and two $[HgX_4]^{2-}$ anions (Figure 1). The interatomic distances and angles are given in Table III. Atoms Hg1 and Hg2 from the complex cations are covalently bound to two thione-sulphur atoms [Hg–S in the range 2.353(3)–2.364(3) in **1** and 2.359(4)–2.370(4) Å in **2**]. These Hg–S bonds are slightly longer than the sum of the covalent radii for linear Hg and S (1.30 + 1.04 Å),[38–40] which is a consequence of additional interactions with the X atoms from the $[HgX_4]^{2-}$ anions. Slight deviations from linearity [S–Hg–S 173.25(12) and 175.63(11) in **1** and 172.22(15) and 177.26(15)° in **2**] are also caused by these weak Hg···X interactions. Both Hg1 and Hg2 have four contacts in the range 3.090(3)–3.470(3) Å in **1** and 3.201(2)–3.504(2) Å in **2**. These contacts are shorter than the sum of the van der Waals radii of Hg and X[38–42] and complete the effective 2+4 coordination sphere,[39,40] forming distorted octahedra around atoms Hg1 and Hg2. In this way, the cations and the anions are interconnected and form a puckered plane parallel to (1 0 0). This two-dimensional network is shown in Figure 2. The Hg···X contacts are weak and have only slight influence on the characteristic linear coordination of mercury and the Hg–S bond length. This can be seen by comparing the bond length in another linear S-coordinated complex, bis[*N*-(propionyl-2-thiolato-*S*)glycine]mercury(II) [Hg–S 2.3414(18) Å, S–Hg–S 180°, two weak Hg···O contacts (effective coordination 2+2)].[43] A 2+4 effective coordination is found in bis(thioacetamide)mercury(II) chloride[44] where two S-bound ligands are at a distance of 2.394(4) Å and four Hg···Cl contacts are in the range 3.067(4)–3.071(5) Å. These two Hg–S bonds of 2.394(4) Å are longer than in **1** and **2** since the contacts in the bis(thioacetamide)mercury(II) chloride are stronger than in **1** and **2**.

The Hg3 and Hg4 atoms from the $[HgX_4]^{2-}$ anions are tetrahedrally coordinated by halogen atoms with the Hg–X bond distances in the range 2.421(3)–2.538(3) Å for Hg–Cl in **1** and 2.552(2)–2.647(2) Å for Hg–Br in **2**.

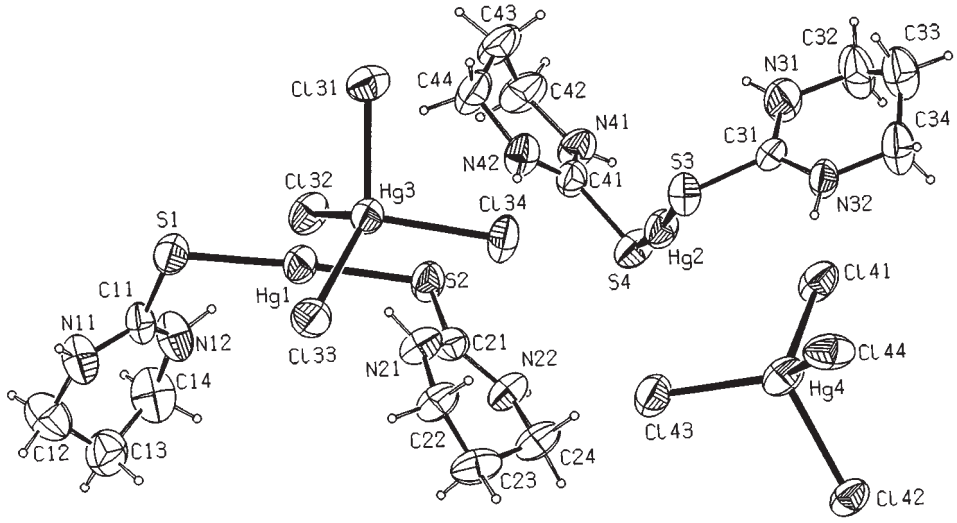

Figure 1. PLATON98 drawing of **1** showing $[Hg(H_4pymtH)_2]^{2+}$ cations and $[HgCl_4]^{2-}$ anions with the atom numbering scheme. The thermal ellipsoids are at the 50% probability level for the non-H atoms. H atoms are shown as spheres of arbitrary radii. **2** is isostructural and has the same atom numbering scheme.

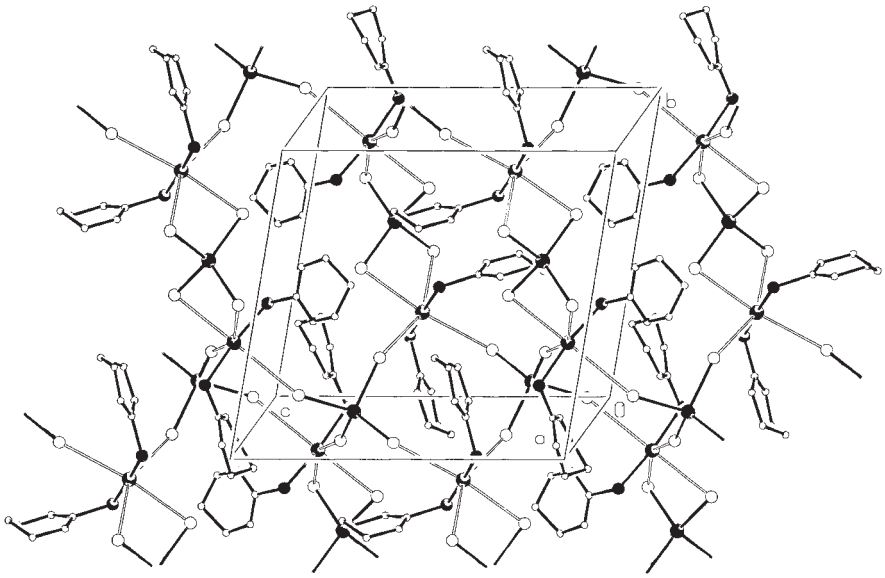

Figure 2. A sheet of $Hg(H_4pymtH)_2]^{2+}$ cations and $[HgCl_4]^{2-}$ anions in **1** interconnected by Hg···Cl contacts (shown by double lines). **2** is isostructural. H atoms are omitted for clarity.

TABLE III

Selected bond distances, contacts / Å and angles / ° for **1**, **2** and H_4pymtH

	$[Hg(H_4pymtH)_2][HgCl_4]$ **1**	$[Hg(H_4pymtH)_2][HgBr_4]$ **2**	H_4pymtH
	Bond distances and contacts / Å		
Hg1-S1	2.360(3)	2.369(4)	
Hg1-S2	2.353(3)	2.359(4)	
Hg2-S3	2.364(3)	2.370(4)	
Hg2-S4	2.355(3)	2.367(4)	
Hg3-X31[a]	2.468(3)	2.601(2)	
Hg3-X32	2.529(3)	2.627(2)	
Hg3-X33	2.421(3)	2.552(2)	
Hg3-X34	2.496(3)	2.608(2)	
Hg4-X41	2.498(3)	2.614(2)	
Hg4-X42	2.538(3)	2.647(2)	
Hg4-X43	2.479(4)	2.602(2)	
Hg4-X44	2.469(3)	2.595(2)	
Hg1··X32	3.090(3)	3.210(2)	
Hg1··X42	3.152(3)	3.299(2)	
Hg1··X44	3.109(3)	3.220(2)	
Hg1··X33[i]	3.276(3)	3.324(2)	
Hg2··X31[ii]	3.470(3)	3.504(2)	
Hg2··X34[iii]	3.070(4)	3.201(2)	
Hg2··X41	3.021(4)	3.131(2)	
Hg2··X43	3.114(3)	3.273(2)	

S1-C11	(S-C1 in H_4pymtH)	1.763(11)	1.732(16)	1.720(2)
S2-C21		1.728(12)	1.758(15)	
S3-C31		1.746(11)	1.729(15)	
S4-C41		1.732(12)	1.721(15)	
Nsp^2-Csp^2 (av.)[b]	(N-C1 in H_4pymtH)	1.318(10)	1.319(6)	1.3311(15)
Nsp^2-Csp^3 (av.)[b]	(N-C2 in H_4pymtH)	1.459(4)	1.459(7)	1.4631(17)
Csp^3-Csp^3 (av.)[b]	(C2-C3 in H_4pymtH)	1.469(21)	1.488(25)	1.510(2)

	Bond angles / °	
S1-Hg1-S2	175.63(11)	177.26(15)
S3-Hg2-S4	173.25(12)	172.22(15)
X31-Hg3-X32	101.59(11)	102.68(6)
X32-Hg3-X33	106.53(12)	107.80(6)
X33-Hg3-X34	108.20(13)	107.17(6)
X31-Hg3-X34	99.30(12)	100.62(7)
X32-Hg3-X34	112.47(11)	115.38(6)
X31-Hg3-X33	128.49(12)	123.58(7)
X41-Hg4-X42	109.78(10)	110.23(6)
X42-Hg4-X43	106.34(11)	107.19(6)
X41-Hg4-X44	114.99(11)	115.64(6)
X42-Hg4-X44	99.29(11)	100.83(6)
X41-Hg4-X43	99.55(12)	101.43(6)
X43-Hg4-X44	126.26(14)	121.25(7)

[a] X = Cl in **1**, Br in **2**.

[b] The standard uncertainties of the average values of bond distances in **1** and **2** have been calculated as $\sigma(\overline{d}) = [\Sigma(d-\overline{d})^2/n(n-1)]^{1/2}$; Symmetry transformations used to generate equivalent atoms: i = $-x,2-y,1-z$; ii = $-x,1-y,-z$; iii = $x,-1+y,z$.

All halogen atoms are involved in additional contacts with atoms Hg1 and Hg2, causing deformation of the HgX_4 tetrahedra [Cl–Hg–Cl 99.29(11)–128.49(12)° in **1** and Br–Hg–Br 100.62(7)–123.58(7)° in **2**]. The $[HgCl_4]^{2-}$ anion is not uncommon and 25 structures containing this anion have been found in the Cambridge Crystallographic Database (CSD).[45] The 154 Hg–Cl bond lengths observed are in the range 2.378–2.860 Å [mean value 2.497(5) Å] and the angles are in the range 92.02–150.85° [mean value 109.3(7)°]. Yet, there are only 5 structures with the $[HgBr_4]^{2-}$ anion [23 Hg–Br bond lengths are in the range 2.560–2.644 Å, mean value 2.598(4) Å; Br–Hg–Br ranges from 103.09 to 113.67°, mean value 109.6(5)°].

The structures of **1** and **2** are, at present, unique cases where isostructurallity was found in such complex polymeric structures with $[HgCl_4]^{2-}$ or $[HgBr_4]^{2-}$ anions as interconnecting units.

All nitrogen H atoms and all halogen atoms, except for X41 (X = Cl^-, Br^-), are involved in hydrogen bond formation of the type N–H···X, ranging

TABLE IV

Hydrogen bond geometry in **1**, **2** and H_4pymtH

D–H···A	*d*(H···A) / Å		∠DHA / °		*d*(D···A) / Å	
	$[Hg(H_4pymtH)_2]\,[HgX_4]$[a]					
	1	**2**	**1**	**2**	**1**	**2**
N11–H11···X43^{i}	2.579	2.755	148	150	3.338(12)	3.526(15)
N12–H12···X42	2.376	2.535	174	171	3.233(11)	3.386(17)
N21–H21···X32	2.375	2.541	175	175	3.233(11)	3.398(14)
N22–H22···X33^{ii}	2.431	2.613	149	143	3.200(11)	3.340(14)
N31–H31···X31^{iii}	2.359	2.462	162	166	3.186(13)	3.303(13)
N32–H32···X44	2.507	2.641	144	139	3.246(11)	3.340(11)
N41–H41···X31^{iv}	2.359	2.469	164	164	3.195(11)	3.302(14)
N42–H42···X34^{v}	2.391	2.559	178	177	3.251(11)	3.418(14)
	H_4pymtH					
N–H1N···S^{vi}[b]	2.48(2)		169.1(16)		3.352(2)	

[a] X = Cl in **1**, Br in **2**.

[b] The N–H distance is 0.88(2) Å. Symmetry code: i = –*x*, 1–*y*, 1–*z*; ii = 1+*x*, *y*, *z*; iii = –*x*, 1–*y*, –*z*; iv = 1+*x*, –1+*y*, *z*; v = *x*, –1+*y*, *z*; vi = 1/2–*x*, *y*, 1/2–*z*.

from 3.186(13) to 3.338(12) Å in **1** and from 3.302(14) to 3.526(15) Å in **2**. The hydrogen bonds are given in Table IV. Five out of eight different hydrogen bonds interconnect atoms within the 2-D planes described earlier, while the others are between these planes and form a 3-D network.

Crystal Structure of H_4pymtH

The structure of the ligand itself, shown in Figure 3, has been known for many years.[31] The first set of data was collected at low temperature in the range 140 to 150 K while the present one at room temperature. Geometry of the molecule is retained but with greater accuracy in this rerefinement. It is interesting to see the structural changes of the ligand molecule after complexation.

According to CSD, the uncoordinated C=S (including delocalized C–S) distance ranges from 1.578 to 1.751 Å for the structural fragment $(X_2N)_2C{=}S$ (X = any atom), *i.e.* thiourea derivatives (the mean value is 1.669(1) Å for 1094 such fragments in 425 structures). The C=S bond in H_4pymtH of 1.720(2) Å is slightly longer than the mean value, but can still be regarded as a thioketo bond. The percentage of the π character is approx. 40%.[46] Due to the aromaticity of the heterocycle, the C=S values in 1,3-imidazole-2-thione derivatives are generally shorter; the longest one of 1.696(5) Å is found in 1,3-dimethyl-4-imidazole-2-thione.[25,47] In contrast, in H_4pymtH delocalization occurs only in the thioamide moiety of the molecule. The C–S, as well as the C–N bond lengths within the thioamide fragment, indicate that aromaticity, *i.e.* planarity of the thioamide fragment, is preserved as a result of the contribution of the zwitterionic resonance form of the thione ligand (Scheme 1).[48] Namely, the Csp^2–Nsp^2 thioamide bond lengths in **1** and **2** (Table III) are mutually similar implying delocalized π-electron density, and slightly shorter than in the H_4pymtH ligand itself, which has the mirror plane symmetry.

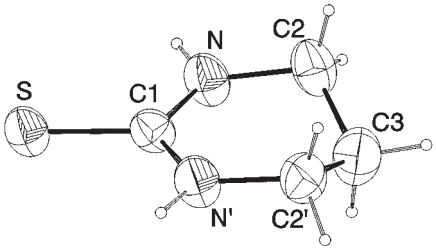

Figure 3. PLATON98 drawing of H_4pymtH with the atom numbering scheme. The thermal ellipsoids are at the 50% probability level for the non-H atoms. H atoms are shown as spheres of arbitrary radii. Atoms C2' and N' are generated by the mirror plane symmetry (*–x, y, z*).

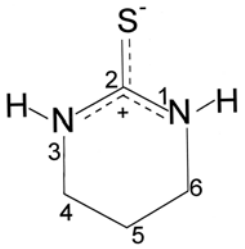

Scheme 1

A tendency to lengthening of the C–S bond upon complexation has been observed in both complexes, **1** and **2**, whereas the thioamide C–N bond is somewhat longer in the free ligand (Table III). These structural changes are in relation with the observed frequency shifts in the IR data.

^{1}H and ^{13}C NMR Spectra

^{1}H and ^{13}C NMR data of the thione molecule (H_4pymtH) and its 1:1 complexes with mercury(II) halides and pseudohalides **1**–**5** are given in Table V. The enumeration of carbon atoms is displayed in Scheme 1. In ^{1}H spectra, the greatest complexation shifts ($\Delta\delta$) are observed for the NH (H-1,3) protons. These protons, which are four bonds away from the mercury, are more deshielded in the complexes than in the ligand molecule. Deshielding of the H-1,3 protons in the 1:1 complexes is greater (by 0.19 to 0.44 ppm) than that previously found in the 1:2 complexes.[25] It was observed that $\Delta\delta$ at the H-1,3 decreases with decreasing electronegativity of halogen atom irrespective of the stoichiometry of the complexes.[38] The linear correlation coefficient (r) between $\Delta\delta$ and the halogen atom electronegativity is 0.99 in the 1:1, while it is 0.96 in the 1:2 complexes. The correlation of $\Delta\delta$ with Taft's σ_I constant of halogens[49] is also better in the 1:1 (r = 0.99) than in the 1:2 (r = 0.93) complexes. The difference in deshielding of NH and the small variations in correlation coefficients of the 1:1 and 1:2 complexes are connected to the structural differences of these two types of complexes. In contrast, differences in deshielding complexation effects of the 1:1 in comparison with the 1:2 complexes are rather small (0.01–0.04 ppm) for the other protons (H-4,6 and H-5).

In ^{13}C NMR spectra, the greatest change upon complexation with mercury was observed in the chemical shift of the thione carbon atom (C–2) since it is the closest to the complexation site. In complexes **1**–**5**, the C–2 is shielded from –4.29 to –9.99 ppm, as compared to the C-2 in parent H_4pymtH. The shielding of the C-2 is in agreement with the decreasing of the C–S bond order and causes a lowering of the paramagnetic contribution

TABLE V

^{1}H and ^{13}C NMR data for the H_4pymtH ligand and its mercury(II) 1:1 complexes **1–5**. Chemical shifts (δ/ppm),[a] H–H spin-spin coupling constants (J_{HH}/Hz),[b] mercury induced ^{1}H shifts ($\Delta\delta$/ppm)[c] and mercury induced ^{13}C shifts ($\Delta\delta$/ppm)[d]

Molecule		H_4pymtH	$HgCl_2(H_4pymtH)$ (**1**)	$HgBr_2(H_4pymtH)$ (**2**)	$HgI_2(H_4pymtH)$ (**3**)	$Hg(SCN)_2(H_4pymtH)$[e] (**4**)	$Hg(CN)_2(H_4pymtH)$[f] (**5**)
	δ	7.86 (2H)	9.22 (2H)	9.13 (2H)	9.03 (2H)	9.27 (2H)	8.41 (2H)
H-1,3	J_{HH}	(s)	(s)	(s)	(s)	(s)	(s)
	$\Delta\delta$		1.36	1.27	1.17	1.41	0.55
	δ	3.09 (4H)	3.30 (4H)	3.29 (4H)	3.29 (4H)	3.31 (4H)	3.21 (4H)
H-4,6	J_{HH}	(m)	(m)	(m)	(m)	(m)	(m)
	$\Delta\delta$		0.21	0.20	0.20	0.22	0.12
	δ	1.71 (2H)	1.83 (2H)	1.83 (2H)	1.85 (2H)	1.85 (2H)	1.76 (2H)
H-5	J_{HH}	5.70 (qn)	4.98 (t)[g]	4.74 (t)[g]	5.56 (qn)	4.98 (t)[g]	4.70 (t)[g]
	$\Delta\delta$		0.12	0.12	0.14	0.14	0.05
C-2	δ	175.95	166.16	166.66	167.78	165.96	171.66
	$\Delta\delta$		–9.71	–9.29	–8.17	–9.99	–4.29
C-4,6	δ	39.88	40.20	40.20	40.25	40.21	40.03
	$\Delta\delta$		0.32	0.32	0.37	0.33	0.15
C-5	δ	19.29	18.05	18.11	18.36	17.91	18.59
	$\Delta\delta$		–1.24	–1.18	–0.93	–1.38	–0.70

[a] Measured in DMSO-d_6 solutions. Referred to TMS. Number of protons in brackets; [b] Digital resolution ±0.32 Hz; (s) singlet, (t) triplet, (qn) quintet, (m) multiplet splitting; [c] Mercury induced ^{1}H shifts are defined as the difference of proton chemical shifts in the complex and free H_4pymtH molecule. Minus sign denotes shielding; [d] Mercury induced ^{13}C shifts are defined as the difference of carbon chemical shifts in the complex and free H_4pymtH molecule. Minus sign denotes shielding. Digital resolution ±0.70 Hz; [e] In $Hg(SCN)_2(H_4pymtH)$ the ^{13}C chemical shift of SCN is 120.14 ppm. $\Delta\delta$ is 4.26 ppm as referred to $Hg(SCN)_2$ in DMSO-d_6, δ = 115.88 ppm; [f] In $Hg(CN)_2(H_4pymtH)$ the ^{13}C chemical shift of CN is 145.00 ppm. It is somewhat broadened. $\Delta\delta$ is 0.25 ppm as referred to $Hg(CN)_2$ in DMSO-d_6, δ = 144.75 ppm; [g] Signal appears as a triplet, since quintet splitting is not completely resolved.

to the shielding constant of the C-2. In the 1:1 complexes, the C-2 is by 1.14 ppm to 2.42 ppm more shielded than in the 1:2 ones, which is related to the differences in their structures. In the 1:1 complexes, $\Delta\delta$ at the C-2 decreases with decreasing electronegativity of the halogen atom, which was previously also found in the 1:2 complexes. Thus, contrary to the decreasing shielding at the C-2, the shielding at the H-1,3 increases from chloro to iodo complex. Both phenomena are connected with the strengthening of the Hg–S bond in the complex, which is due to the change of the character of the Hg–X bond on going from iodo to chloro complex. The linear correlation coefficient between the complexation shift, $\Delta\delta$, at the C-2 and the halogen atom electronegativity is 0.99 (it was 0.98 in 1:2). The correlation coefficient for the relationship between $\Delta\delta$ and Taft's σ_I value of halogen is also 0.99 (the same as in 1:2).

The complexation shifts at the C-5 are greater (–0.70 ppm to –1.38 ppm, shielding effects) than those at the C-4,6 (0.15 to 0.37 ppm, deshielding effects). Although the C-5 is five bonds, while the C-4,6 only four bonds away from mercury, complexation effects at the former carbon are *ca.* three to five times greater than at the latter ones. The same features were found for the corresponding carbons in the 1:2 complexes, but the magnitudes of the complexation effects are slightly greater in the 1:1 than in the 1:2 complexes. The linear correlation coefficient of $\Delta\delta$ with the halogen atom electronegativity at the C-4,6 is 0.92 (it was 0.90 in 1:2), while with Taft's σ_I value of the halogen atoms it is 0.94 (it was only 0.87 in 1:2). The correlation coefficient of $\Delta\delta$ at the C-5 *versus* electronegativity of the halogens is 0.97 (it was 0.98 in 1:2), while that of $\Delta\delta$ *versus* Taft's σ_I constants of the halogens is 0.99 (the same was found in 1:2).

In a 1:1 series of complexes, the greatest ^{1}H complexation shift (1.41 ppm) was observed at the H-1,3 in the thiocyanato complex, while the smallest $\Delta\delta$ (0.55 ppm) in the cyano complex. The same regularity was found in a 1:2 series of complexes, but $\Delta\delta$ in the thiocyanato complex was 1.15 ppm, while in the cyano complex it was 0.36 ppm. The greatest ^{13}C complexation shift in a 1:1 series was detected at the C-2 in the thiocyanato complex (–9.99 ppm), and the smallest one at the C-2 in the cyano complex (–4.29 ppm). In a 1:2 series, the values for the thiocyanato and cyano complexes were –8.85 ppm and –2.96 ppm, respectively.

Accordingly, one can say that trends and regularities in ^{1}H and ^{13}C chemical and complexation shifts in both series of the 1:1 and 1:2 complexes are similar, but the magnitudes of changes are different.

The NMR data show that, in a saturated carbon atom framework, carbon atoms are sensitive to mercury binding even if they are five bonds away from mercury and hence long-range shifts may also be useful for complexa-

tion monitoring. Long-range complexation shifts result both from conformational changes and generation of positive charge in the parent H_4pymtH ring upon its mercuration, which in turn induces subtle electron redistribution throughout the molecule, with sign alternation of mercuration shifts.

However, changes of chemical shifts of the NH (four bonds) and the C-2 (two bonds) are the most reliable complexation tests, reflecting also the difference in the structures of the 1:1 and 1:2 complexes.

*Structures of $HgI_2(H_4pymtH)$ (**3**), $Hg(SCN)_2(H_4pymtH)$ (**4**) and $Hg(CN)_2(H_4pymtH)$ (**5**)*

The crystals of **3** were much smaller than those of **1** and **2** and only a limited data set could be obtained on the PW1100 diffractometer. A preliminary structure determination reveals that the structure of **3** is quite different from **1** and **2** and that it is built up of molecules of $HgI_2(H_4$pymtH). Hg is surrounded by the S atom from the H_4pymtH ligand and by two I atoms, forming a trigonal coordination sphere.

Crystals of **4** and **5** were twinned and a good data set could not be obtained. In predicting molecular structures, weak interactions have to be taken into account. These do not have to be the same in solid and in solution, and an accurate prediction is hardly possible. From the chemical analysis, IR and NMR data, analogy with the 1:2 complexes[25] and data obtained from the CSD, we suppose that in **4** the mercury atom is bonded to three S atoms (two from SCN^- and one from H_4pymtH). An additional weak interaction with the N atom from the thiocyanate of another complex molecule can be assumed. In this way, the N atoms are both bridging and terminal and the possible effective coordination of mercury is 3+1. This type of bonding gives a polymeric structure.[50] The available data for **5** show two strong bonds to CN^- and a weakly S-bound H_4pymtH. The structure could be similar to the complex of mercury(II) cyanide with thiourea[51] where the coordination is 2+4, *i.e.* linearly coordinated cyano ligands and four weak contacts with S-bridging atoms. This is also the only (unfortunately, quite imprecisely, R = 14.1%) determined crystal structure of mercury(II) cyanide with a S-donating ligand. In the $Hg(CN)_2$ structure[37] the coordination is also 2+4 but with Hg···N contacts.

Thermal Analysis (TGA and DTA)

The samples of mercury complexes **1–5** were heated from room temperature up to 700 °C (see thermoanalytical data shown in Table VI). Simultaneous occurrence of different steps of the decomposition process, resulting

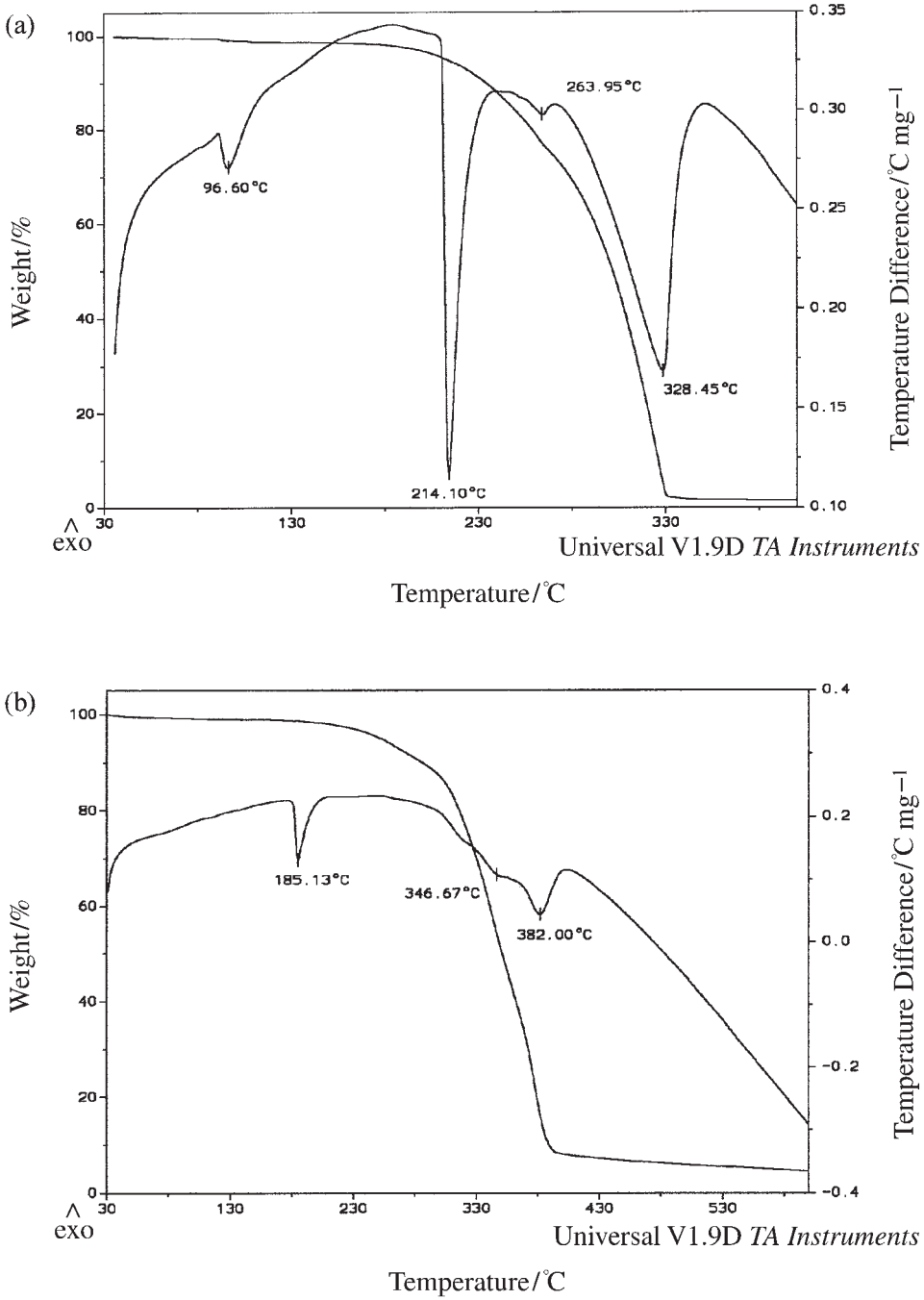

Figure 4. TGA-DTA curves of: (a) H_4pymtH; (b) $HgCl_2(H_4pymtH)$ (**1**).

TABLE VI

Thermoanalytical data for complexes **1**–**5**

Complex	Process	Peak temperature / °C
$HgCl_2(H_4pymtH)$	melting	185.13
(**1**)	I endo	346.00
	II endo	382.33
$HgBr_2(H_4pymtH)$	melting	141.60
(**2**)	I endo	350.29
	II endo	409.56
$HgI_2(H_4pymtH)$	melting	128.26
(**3**)	I endo	337.47
	II endo	427.18
$Hg(SCN)_2(H_4pymtH)$	melting	121.70
(**4**)	I exo	202.28
	II endo	369.22
	III endo	421.38
$Hg(CN)_2(H_4pymtH)$	melting[a]	203.34
(**5**)	I exo	225.44
	II exo	289.12
	III endo	441.79

[a] Decomposition and melting occur simultaneously.

in an overlap of the DTA peaks, disabled the partial determination of the weight loss of possible decomposition products (Figure 4).

The DTA curves were dominated by typical endothermic minima, which correspond to the melting process. The melting of mercury(II) complexes is represented by the first single endothermic peak at a temperature between 120–205 °C. The endothermic peak that corresponds to the melting of the halide complexes progressively decreases with the increasing formula weight. Melting and decomposition take place simultaneously for **5**. Decomposition of the halide complexes is represented by two overlapping endothermic peaks. The first one is small and broad, and the second is larger and sharper. For **3**, the DTA curve contains endothermic minima at 337.47 and 427.18 °C, for **2** the endothermic minima are at 350.29 and 409.56 °C, and for **1** at 346.00 and 382.33 °C. Two different steps of decomposition can be associated with the degradation of the ligand and the residue. From

these results one can recognize the order of decreasing stability as follows: bromo > chloro > iodo complex. The decomposition of **4** is followed by an exothermic peak at 202.28 °C, an endothermic minimum at 369.22 °C, and a very small and broad endothermic peak at 421.38 °C. The DTA curve of **5** is characterized by three peaks, two overlapping exothermic peaks, a sharp one at 225.44 °C, one small and broad at 289.12 °C, and the third one being a broad endothermic peak at 441.79 °C. The first decomposition step determined by (I) and (II) peaks, marked in Table VI, represents elimination of the ligand. From the analysis of TGA-DTA curves of the reactants, the second step, endo(III), is connected with the degradation of the residues.

Supplementary Materials. – Crystallographic data for the structures in this paper have been deposited at the Cambridge Crystallographic Data Centre, 12 Union Road, Cambridge CB2 1EZ, UK (fax: +44-1223-336033; E-mail: deposit@ccdc.cam.ac.uk) and can be obtained on request, free of charge, by quoting the publication citation and the deposition numbers 142800 and 142801 for **1** and **2**, respectively, and 144427 for H_4pymtH. Structure factor tables are available from the authors.

Acknowledgements. – This research was supported by the Ministry of Science and Technology of the Republic of Croatia (Grants No. 119408 and 00980802).

REFERENCES

1. T. L. Blundell and J. Jenkins, *Chem. Soc. Rev.* (1977) 139–171.
2. N. J. Taylor and A. J. Carty, *J. Am. Chem. Soc.* **99** (1977) 6143–6145.
3. M. Sandström, I. Persson, and P. Persson, *Acta Chem. Scand.* **44** (1990) 653–675.
4. I. Persson, K. C. Dash, and Y. Kinjo, *Acta Chem. Scand*. **44** (1990) 433–442.
5. I. Persson, M. Sandström, and P. L. Goggin, *Inorg. Chim. Acta* **129** (1987) 183–197.
6. I. Persson, M. Landgren, and A. Marton, *Inorg. Chim. Acta* **116** (1986) 135–144.
7. I. Persson, M. Sandström, P. L. Goggin, and A. Mosset, *J. Chem. Soc., Dalton Trans*. (1985) 1597–1604.
8. S. Ahrland, *Pure & Appl. Chem*. **54** (1982) 1451–1468.
9. L. G. Sillén, *Acta Chem. Scand*. **3** (1949) 539–553.
10. Y. Marcus, *Acta Chem. Scand.* **11** (1957) 599–609.
11. P. K. Gallagher and E. L. King, *J. Am. Chem. Soc.* **82** (1960) 3510–3514.
12. S. Ahrland, L. Kullberg, and R. Portanova, *Acta Chem. Scand*., *Ser. A* **32** (1978) 251–258.
13. J. J. Christiansen, R. M. Izatt, L. D. Hansen, and J. D. Hale, *Inorg. Chem.* **3** (1964) 130–133.
14. E. S. Raper, *Coord. Chem. Rev.* **61** (1985) 115–184.
15. E. S. Raper, *Coord. Chem. Rev.* **153** (1996) 199–255.
16. E. S. Raper, *Coord. Chem. Rev.* **165** (1997) 475–567.
17. N. Davidović, D. Matković-Čalogović, Z. Popović, and I. Vedrina-Dragojević, *Acta Crystallogr.*, *Sect. C* **54** (1998) 574–576.

18. E. S. Raper, J. R. Creighton, N. A. Bell, W. Clegg, and L. Cucurull-Sánchez, *Inorg. Chim. Acta* **277** (1998) 14–20.
19. Z. Popović, D. Matković-Čalogović, J. Hasić, and D. Vikić-Topić, *Inorg. Chim. Acta* **285** (1999) 208–216.
20. Z. Popović, D. Matković-Čalogović, Ž. Soldin, G. Pavlović, N. Davidović, and D. Vikić-Topić, *Inorg. Chim. Acta* **294** (1999) 35–46.
21. G. Pavlović, Z. Popović, Ž. Soldin, and D. Matković-Čalogović, *Acta Crystallogr., Sect. C* **56** (2000) 61–63.
22. G. Pavlović, Z. Popović, Ž. Soldin, and D. Matković-Čalogović, *Acta Crystallogr., Sect. C* **56** (2000) 801–803.
23. N. A. Bell, W. Clegg, J. R. Creighton, and E. S. Raper, *Inorg. Chim. Acta* **303** (2000) 12–16.
24. N. A. Bell, T. N. Branston, W. Clegg, J. R. Creighton, L. Cucurull-Sánchez, M. R. J. Elsegood, and E. S. Raper, *Inorg. Chim. Acta* **303** (2000) 220–227.
25. Z. Popović, D. Matković-Čalogović, G. Pavlović, Ž. Soldin, M. Rajić, D. Vikić-Topić, and D. Kovaček, *Inorg. Chim. Acta* **306** (2000) 142–152.
26. P. A. Dean, *Prog. Inorg. Chem.* **24** (1978) 109–178.
27. F. W. B. Einstein, C. H. Jones, T. Jones, and R. D. Sharma, *Inorg. Chem.* **22** (1983) 3924–3928.
28. A. Álvarez-Larena, W. Clegg, L. Cucurull-Sánchez, P. Gonzàlez-Duarte, R. March, J. F. Piniella, J. Pons, and X. Solans, *Inorg. Chim. Acta* **266** (1997) 81–90.
29. N. A. Bell, M. Goldstein, T. Jones, and I. W. Nowell, *Inorg. Chim. Acta* **48** (1981) 185–189.
30. P. Gouverneur and W. Hoedeman, *Anal. Chim. Acta* **30** (1964) 519–523.
31. H. W. Dias and M. R. Truter, *Acta Crystallogr.*, **17** (1964) 937–943.
32. Stoe & Cie, STADI4, Diffractometer Control Program, Darmstadt, Germany, 1995.
33. Stoe & Cie, X-RED, Data Reduction Program, Darmstadt, Germany, 1995.
34. G. M. Sheldrick, *Acta Crystallogr., Sect. A* **46** (1990) 467–473.
35. G. M. Sheldrick, SHELXL97, Program for the Refinement of Crystal Structures, University of Göttingen, Germany, 1997.
36. A. L. Spek, PLATON98 for Windows, University of Utrecht, The Netherlands, 1998.
37. R. C. Seccombe and C. H. L. Kennard, *J. Organometal. Chem.* **18** (1969) 243–247.
38. L. Pauling, *The Nature of the Chemical Bond*, Third Ed., Cornell University Press, Ithaca, NY, 1960.
39. D. Grdenić, *Quart. Rev.* **19** (1965) 303–328.
40. D. Grdenić, *Connections in the Crystal Structures of Mercury Compounds*, in: G. Dodson, J. P. Glusker, and D. Sayre (Eds.), *Structural Studies of Molecules of Biological Interest*, Clarendon Press, Oxford, 1981, pp. 207–221.
41. D. Matković-Čalogović, Ph. D. Thesis (in Croatian; Abstract in English), University of Zagreb, 1994.
42. S. C. Nyburg and C. H. Faerman, *Acta Crystallogr., Sect. B* **41** (1985) 274–279.
43. Z. Popović, D. Matković-Čalogović, J. Hasić, M. Sikirica, and D. Vikić-Topić, *Croat. Chem. Acta* **72** (1999) 279–294.
44. M. Rolies and C. J. De Ranter, *Cryst. Struct. Comm.* **6** (1977) 157–161.
45. Cambridge Structural Database, Version 5.18, Cambridge Crystallographic Data Centre, 12 Union Road, Cambridge, UK, 1999.
46. N. Trinajstić, *Tetrahedron Lett.* **12** (1968) 1529–1532.

47. G. B. Ansell, *J. Chem. Soc., Perkin Trans. 2* (1972) 841–843.
48. E. Binamira-Soriaga, M. Lundeen, and K. Seff, *Acta Crystallogr., Sect. B* **35** (1979) 2875–2879.
49. C. Hansch, A. Leo, and R. W. Taft, *Chem. Rev.* **91** (1991) 165–195.
50. J. Pickardt, G.-T. Gong, and I. Hoffmeister, *Z. Naturforsch.* **B 50** (1995) 993–996.
51. E. Moreno and A. Lopez Castro, *An. Fis.* **67** (1971) 371–381.

SAŽETAK

Preparacija, termička analiza i spektralna karakterizacija 1:1 kompleksa živinih(II) halogenida i pseudohalogenida s 3,4,5,6-tetrahidropirimidin-2-tionom. Kristalne strukture bis(3,4,5,6-tetrahidropirimidin-2-tion-*S*)živina(II) tetrakloro- i tetrabromomerkurata(II)

Zora Popović, Dubravka Matković-Čalogović, Gordana Pavlović, Željka Soldin, Gerald Giester, Maša Rajić i Dražen Vikić-Topić

Dobiveni su živini(II) kompleksi tipa $HgX_2(H_4pymtH)$ (X = Cl^-, Br^-, I^-, SCN^-, CN^-; H_4pymtH = 3,4,5,6-tetrahidropirimidin-2-tion) i strukturno su karakterizirani IR, ^1H i ^{13}C NMR spektroskopijom. Strukture kloro- i bromo- kompleksa određene su röntgenskom strukturnom analizom monokristala i nađeno je da su izostrukturni. Njihove kristalne strukture sastoje se od kompleksnih kationa $[Hg(H_4pymtH)_2]^{2+}$ i kompleksnih aniona $[HgX_4]^{2-}$ koji su kontaktima Hg···X međusobno povezani u naboranu mrežu. Kristalna struktura H_4pymtH određena je do veće točnosti. U NMR spektrima otopina kompleksa pronađen je najveći kompleksacijski efekt za kemijske pomake tioketo-ugljikovih atoma i kemijske pomake NH-protona.